P3.10 MICROPHYSICAL INFLUENCES ON MODELED ARCTIC ROLL CLOUD STRUCTURE

Steven D. Greenberg* and Jerry Y. Harrington
The Pennsylvania State University, University Park, Pennsylvania

1. INTRODUCTION

Roll clouds, and associated roll convection, are fairly common features of the atmospheric boundary layer. While these organized cumuliform clouds are found over many regions of the planet, they are quite ubiquitous near the edge of the polar ice sheets. In particular, during periods of off-ice flow, when cold polar air flows from the ice pack over the relatively warm ocean water, strong boundary layer convection develops along with frequent rolls. According to Brümmer and Pohlman (2000), most of the total cloud cover in the Arctic is due to roll clouds.

In an effort to examine the influences of mixed-phase microphysics on the boundary layer evolution of roll clouds during off-ice flow, Olsson and Harrington (2000) used a 2-D mesoscale model coupled to a bulk microphysical scheme (see section 2). Their results showed that mixed-phase clouds produced more shallow boundary layers with weaker turbulence than liquid-phase cases. Furthermore, their results showed that because of the reduced turbulent drag on the atmosphere in the mixed-phase case, regions of mesoscale divergence in the marginal ice-zone were significantly affected. A follow-up 2-D study (Harrington and Olsson, 2001) showed that the reduced turbulent intensity in mixed-phase cases was due to precipitation. Ice precipitation caused downdraft stabilization which fed back and caused a reduction in the surface heat fluxes.

Fully 3-D LES studies of roll convection have begun to separate important causal relationships (see Glendening, 2000). Chlond's (1992) liquid cloud studies showed that condensation is vital to the maintenance of turbulent intensity and cloud structure. Furthermore, their simulations suggest that radiative cooling, subsidence, and variation in surface temperature all importantly affected turbulent intensity. Rao and Agee (1996) used a LES to simulate mixed-phase cloudy convection. Their comparison of liquid and mixed-phase cloud boundary layer convection showed that turbulent intensity is weaker and skewness is greater in the mixed-phase case. Furthermore, this work showed that the mixed-phase case produced 2-D roll like convection whereas the liquid case produced spoke-like convection.

In this work, we extend the work of Olsson and Harrington (2000) and Harrington and Olsson (2001) by examining the impacts of ice microphysics on roll convection. We will present results that illustrate how microphysics alters roll cloud structure and dynamics.

*corresponding author address: Steven Greenberg, Department of Meteorology, Penn State University, University Park, PA, 16802. email: stegreen@psu.edu

2. NUMERICAL MODEL AND CASE

The numerical model used is the LES version of the Regional Atmospheric Modeling System (RAMS) with the bulk microphysics of Walko et al. (1995). This model predicts the evolution of seven different liquid and ice hydrometeor species as well as water vapor. The microphysics is coupled to the radiation scheme of Harrington and Olsson (2000) which includes scattering and absorption by liquid and ice.

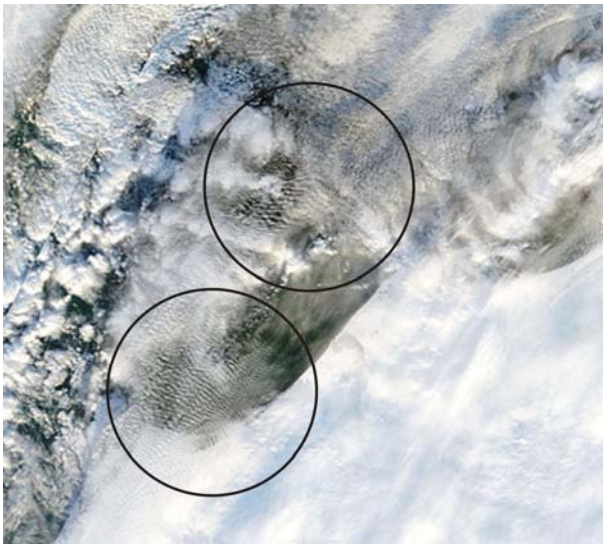

Figure 1. Satellite image of roll clouds near the North Slope of Alaska during M-PACE.

The case used for the simulations was observed during the Mixed-Phase Arctic Cloud Experiment which took place on the North Slope of Alaska in October 2004. Off-ice flow in the vicinity of a marginal ice zone produced organized convection in the form of roll clouds. Figure 1 shows a satellite image of roll clouds from a time during the experiment at the northern coast of Alaska.

3. ANALYSIS

The RAMS model was arranged with a horizontal domain size of 8 by 17 km. The grid-spacing used was 120 m in the horizontal and 40 m in the vertical. To emulate the effects of off-ice flow, the lower SST boundary of the model was warmed using the SST-gradient given by Lüpkes and Schlünzen (1996).

Only two cases were simulated because of the intense computational costs. The first case used only

liquid-phase microphysics with no sedimentation (case LP) whereas the second case used mixed-phase microphysics with sedimentation (case MP). Both cases produced horizontal roll cloud convection followed later by cellular convection.

3.1 Snapshots of Model Fields

Figure 2 shows snapshots of the total water path (WP) and average vertical motion (*w*) for case LP and MP after 1 hour of simulation time. At this time, roll convection has developed along with distinct quasi-lineal roll clouds. The boundary layer is 1 km deep and the average vertical motions are of approximately equal magnitude for both cases. Perhaps the most obvious difference between the two simulations is that updrafts are cloudy whereas downdrafts are dry only in the MP simulation. The case with liquid-only clouds (LP) produces essentially 100% cloud fraction and the rolls are recognizable as locally high regions of WP collocated with updrafts. This basic difference, dry downdrafts in MP and moist downdrafts in LP, is characteristic of the entire simulation. As Olsson and Harrington (2000) and Harrington and Olsson (2001) have shown, the dry downdrafts in MP are due to ice precipitation which falls predominately, and continually, from updrafts.

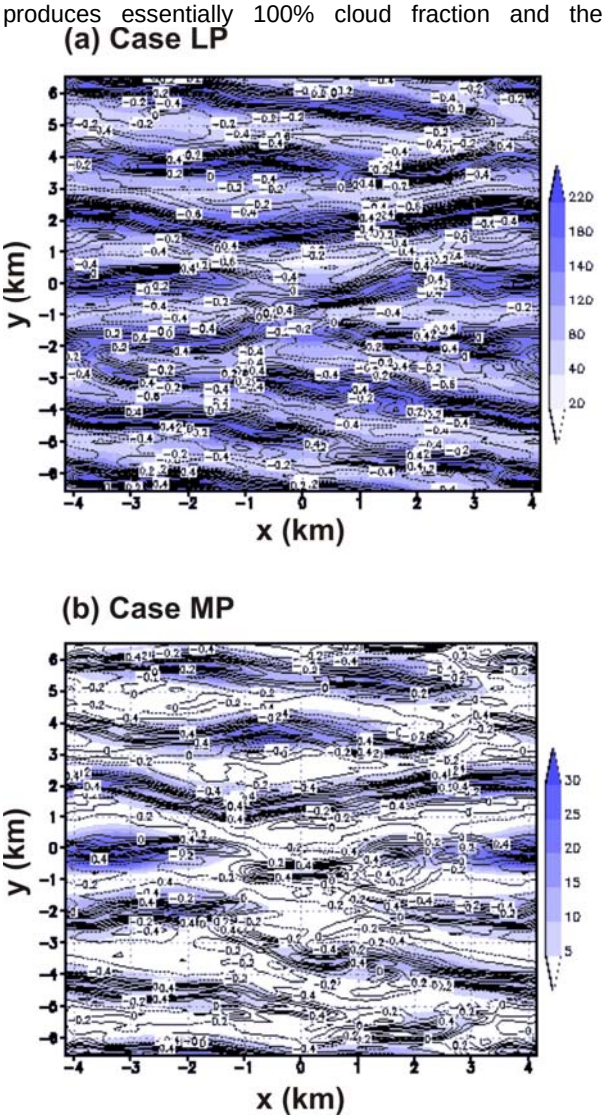

Figure 2. Total water path (g m^{-2}, shaded) and average vertical motion (m s^{-2}, contour).

3.2 Analysis of Case Evolution

Temporal evolution of the WP for both cases is shown in Figure 3. Similar to Olsson and Harrington's (2000) simulations, the WP in case LP develops rapidly and continues to increase throughout the simulation. Clouds develop initially in case MP; however this water is quickly precipitated to the surface. After approximately 100 minutes of simulation time cloudiness increases rapidly in MP. This delay in the onset of persistent cloud cover is due to the fact that ice precipitation significantly warmed the boundary layer in the first 30 minutes. As might be expected, P_i increases concurrently with WP in the mixed-phase case. Note that after about 150 minutes of simulation time, the WP in case MP is fairly steady as are the precipitation rates. This result stands in stark contrast to the 2-D simulation results presented by Olsson and Harrington (2000) which showed that precipitation causes large oscillations in the WP field. However, Harrington and Olsson (2001) showed that the above steady-WP situation is strongly dependent on ice-nuclei concentrations and feedbacks with surface heat fluxes.

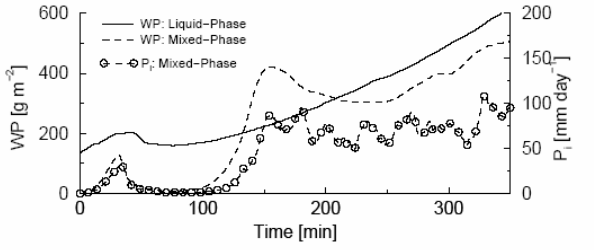

Figure 3. Time-series of total water path (WP) for MP and LP and instantaneous precipitation rate (P_i) for MP.

The dynamics of the roll convection are strongly modulated by ice precipitation as is shown in Figure 4. The domain averaged vertical component of TKE $\langle w'w' \rangle$ and the domain averaged total TKE $0.5\left(\langle u'u' \rangle + \langle v'v' \rangle + \langle w'w' \rangle\right)$ for two different times is shown for both cases. Figure 4a illustrates the vertical and total TKE 40 minutes into the simulation. At this time precipitation and WP have returned to almost zero in MP whereas WP for LP remains greater. The onset of precipitation before this time suggests stronger boundary layer circulations as is indicated by the MP vertical and total TKE being greater at every height

compared to LP. This is the case for all times during the onset of the first precipitation event.

In contrast to this result, Figure 4b portrays an opposite picture. At 60 minutes into the simulation, the vertical and total TKE for MP is less than LP at every height. This result is dominant throughout the rest of the simulation indicating weaker BL circulations in MP. In fact, the convective velocity scale for MP is roughly 7 m s^{-1} whereas it is 4 m s^{-1} in case LP. Using 2-D simulations, Harrington and Olsson (2001) show that this reduction in vertical TKE is due to two coupled processes. First, the buoyancy of downdrafts is reduced by precipitation warming in MP. Second, the sensibly warmed boundary layer and reduced surface winds (through reduced momentum fluxes) produce weaker sensible heat fluxes out of the surface in case MP. This is also the case for these 3-D roll cloud simulations as is shown in Figures 5 and 6.

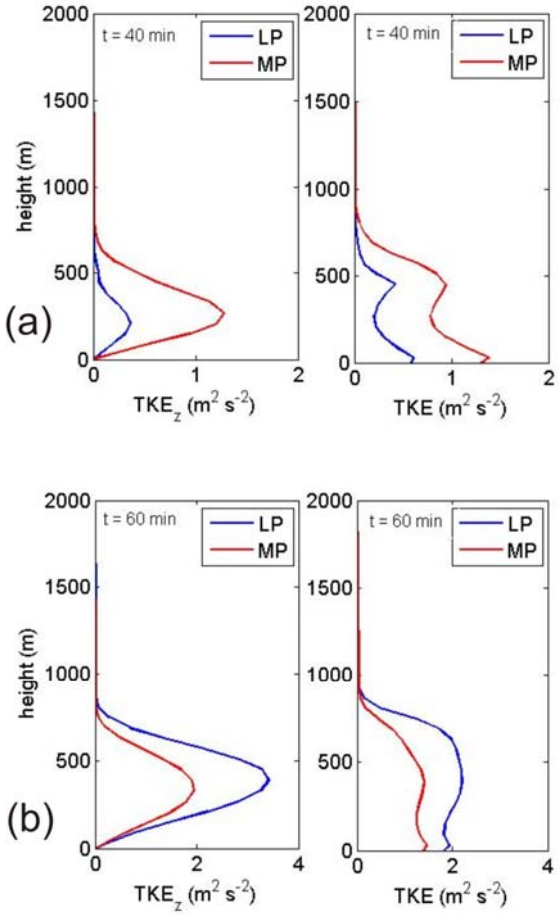

Figure 4. Vertical and Total TKE profiles for LP and MP cases at (a) t = 40 min and (b) t = 60 min.

Figure 5 exhibits the buoyancy flux partitioned between updrafts and downdrafts, for LP and MP. Figure 5a shows these values for 40 minutes into the simulation (as in Figure 4a) and Figure 5b shows the same for 60 minutes into the simulation (as in Figure 4b). For the most part, updrafts at both time periods create positive buoyancy flux (negative at cloud top due to entrainment) while downdraft buoyancy fluxes vary with height. However, the updraft buoyancy flux for MP at any time is dependent on the onset of initial precipitation. The buoyancy flux for MP updrafts in Figure 5a is greater than that of LP due to the initial stronger boundary layer circulation induced by MP. Updrafts then experience a reduction in buoyancy through excessive precipitation loading and a reduction in surface heat fluxes. As Harrington and Olsson (2001) have shown, ice precipitation sensibly warms and dries updrafts which is eventually realized as a buoyancy consumption within downdrafts. In the fully 3-D case presented here, this buoyancy consumption mechanism is not as prevalent within downdrafts; instead buoyancy fluxes are nearly zero throughout most of the simulation

The consumption of TKE generated by ice precipitation has a significant impact on the surface heat fluxes. As Figure 6 shows, sensible heat fluxes

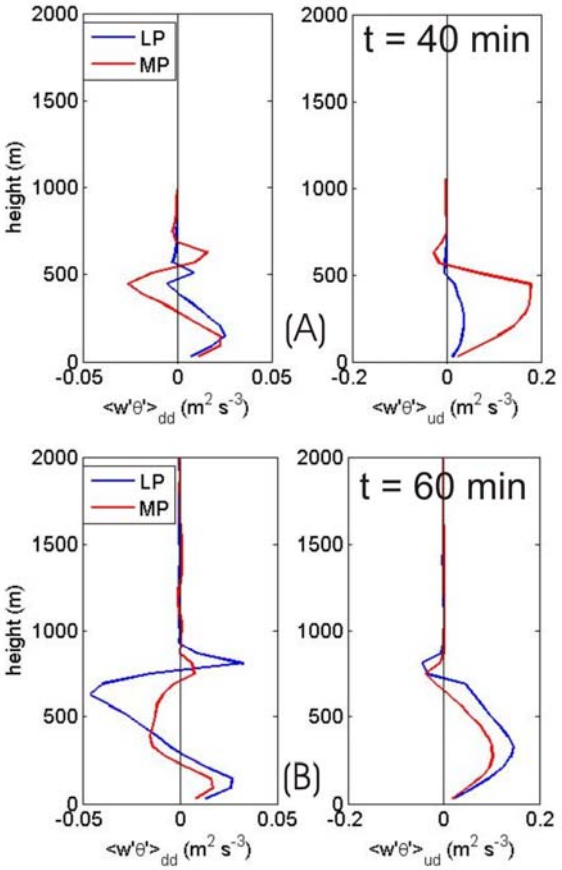

Figure 5. Updraft and downdraft buoyancy fluxes for LP and MP cases at (a) t = 40 min and (b) t = 60 min.

are reduced by 10 – 40 W m^{-2} whereas latent heat fluxes are increased by 5 – 20 W m^{-2} in case MP. The sensible heat fluxes at the surface are reduced because the BL in case MP is warmed through ice precipitation.

This makes the temperature difference between the atmosphere and ocean surface smaller. Latent heat fluxes, however, have increase in case MP because the atmosphere is dried and warmed (relative to case LP) through ice precipitation.

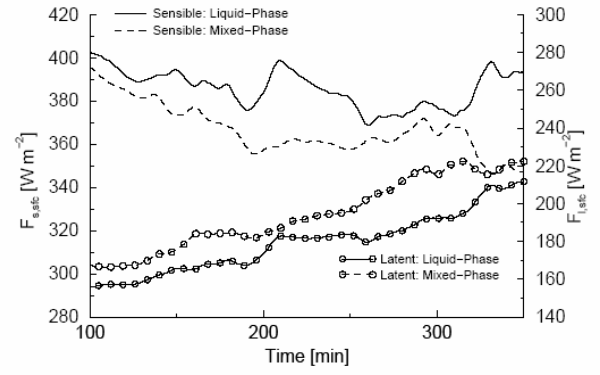

Figure 6. Time-series of sensible and latent heat fluxes.

Thus, there appears to be a positive feedback between direct ice precipitation reduction of TKE and indirect reductions in TKE through smaller surface heat fluxes. These results are in general agreement with the 2-D simulations of Harrington an Olsson (2001).

4. SUMMARY AND FUTURE WORK

In this study, we used the LES mode of the RAMS model with explicit microphysics to examine the influence of ice-phase processes on roll cloud development and dynamics. This study was conducted, in part, because Harrington and Olsson (2001) found that ice-phase processes strongly affected the evolution of the cloud boundary layer over the marginal ice zone. However, those results were 2-D and, hence, did not capture the roll dynamics prevalent in the observed case.

Our studies show that the processes discussed in Harrington and Olsson (2001) appear to occur, in a weaker sense, in the fully 3-D simulations. Ice precipitation from mixed-phase clouds produces dry downdraft regions and true roll clouds. The TKE is reduced in the mixed-phase case through ice precipitation which stabilizes downdrafts and reduces surface sensible heat fluxes.

A complete investigation of these simulations will be accomplished with careful attention to the underlying dynamics of roll cloud formation, evolution, and destruction. In future work, this study will include spectral analysis to determine how the dominant scales vary in space and time as well as a more detailed discussion of the TKE budget terms. This information will be used to provide a more complete picture the dominant cloud feature over the Arctic marginal ice zone.

5. REFERENCES

Brummer, B. and S. Pohlmann, 2000: Wintertime roll and cell convection over Greenland and Barents Sea regions: A climatology. *J. Geophys. Res.*, 105, 15559-15566.

Chlond, A., 1992: Three-dimensional simulation of cloud street development during a cold air outbreak. *Bound.-Layer Meteor.*, 58, 161-200.

Glendening, J. W., 2000: Budgets of lineal and nonlineal turbulent kinetic energy under strong shear conditions. *J. Atmos. Sci.*, 57, 2297-2318.

Harrington, J. Y. and P. Q. Olsson, 2001: On the potential influence of ice nuclei on surface-forced marine stratocumulus cloud dynamics. *J. Geophys. Res.*, 106, 27473-27484.

Kottmeier, C., J. Hartmann, C. Wamser, A. Bochert, C. Lupkes, D. Freese, and W. Cohrs, 1994: Radiation and eddy flux experiment 1993 (REFLEX II). *Berichte zur Polar-und Meeresforschung*.

Lupkes, C. and K. H. Schlunzen, 1996: Modelling the arctic convective boundary-layer with different turbulence parameterizations. *Bound.-Layer Meteor.*, 79, 107-130.

Olsson, P. Q. and J. Y. Harrington, 2000: Dynamics and energetics of the cloudy boundary layer in simulations of off-ice flow in the marginal ice zone. *J. Geophys. Res.*, 105, 11889-11899.

Rao, G. S. and E. M. Agee, 1996: Large eddy simulation of turbulent flow in a convective boundary layer filled with snow. *J. Atmos. Sci.*, 53, 86-100.

Walko, R. L., W. R. Cotton, M. P. Meyers, and J. Y. Harrington, 1995: New RAMS cloud microphysics parameterization, Part I: the single-moment scheme. *Atmos. Res.*, 38, 29-62.